Influence of galaxy rotation and outflows in the Lyman Alpha spectral line

Maria Camila Remolina Gutiérrez

A monograph presented for the degree of
Physicist

Departamento de Física
Facultad de Ciencias
Universidad de los Andes
Colombia

November, 2015

Dedicated to

Someone here

Influence of galaxy rotation and outflows in the Lyman Alpha spectral line

Maria Camila Remolina Gutiérrez

Submitted for the degree of Physicist
November, 2015

Abstract

Your abstract here Your abstract here

Declaration

The work in this monograph is based on research carried out at the Physics Department of Universidad de los Andes, Colombia. No part of this work has been submitted elsewhere for any other degree and it is all my own work unless referenced to the contrary in the text.

Acknowledgements

We acknowledge Alvaro Orsi and Julian Mejia for collaborating with us offering their time, advice and especially data. We used their outflow simulations in order to get our results in the appendix.

Most of our code benefits from the work of the IPython and Matplotlib communities ([1, 2]).

The data, source code and instructions to replicate the results of this monograph can be found on `https://github.com/astroandes/CLARA_RotationOutflows`.

MISSING:

- More acknowledgments.

Contents

Chapter 1

Introduction

Galaxies are one of the most important structures in the universe. They are key to understand it and its evolution. So far, human kind has been able to study really well our close galaxies. However, the young ones are very far away and only a point of light reaches our telescopes. This point, although tiny, contains information of millions of stars and space material that could unravel many mysteries. For example, it could explain how our own Milky Way was created. So, it is our challenge as scientists to obtain as much information as possible from it. This task can be fulfilled in many different ways. The purpose of this monograph is to become one of these solutions.

1.1 Lyman Alpha Emitters

It has been discovered that young galaxies in the universe are common to have a lot of Hydrogen (H) atoms. Also, that the material inside of them is easily ionized. These two facts leave the H atoms prone to excite.

When a Hydrogen atom is excited, the only electron it has moves to a higher energy level. However, a short time passes until it is no longer able to maintain itself in this state. For this, the electron goes back to the ground level it was before. Finally, as the energy obtained from this excitement has to be conserved, it is

emitted as a particle of light, called a photon, with a wavelength of 1215.67 $\mathring{A}$. This light emission process is called the Lyman Alpha (Ly-α) radiation, discovered by Theodore Lyman in 1906.

This Ly-α radiation happens in all the H atoms in the galaxy. Due to the amount of atoms inside it, the whole body becomes a strong Ly-α radiator, and the galaxy is now called a Lyman Alpha Emitter (LAE).

When astronomers observe a LAE they decompose its incoming light in different wavelengths and make a histogram of them. This distribution is called the spectrum of the galaxy. If now I look at the range of the spectrum around the Ly-α wavelength there is a clear and strong emission called the Ly-α line. However, the line is not a single peak at 1215.67 $\mathring{A}$ as one would first expect, but it bestrews around this wavelength in a particular shape. This morphology depends mostly on the galaxy's dynamics.

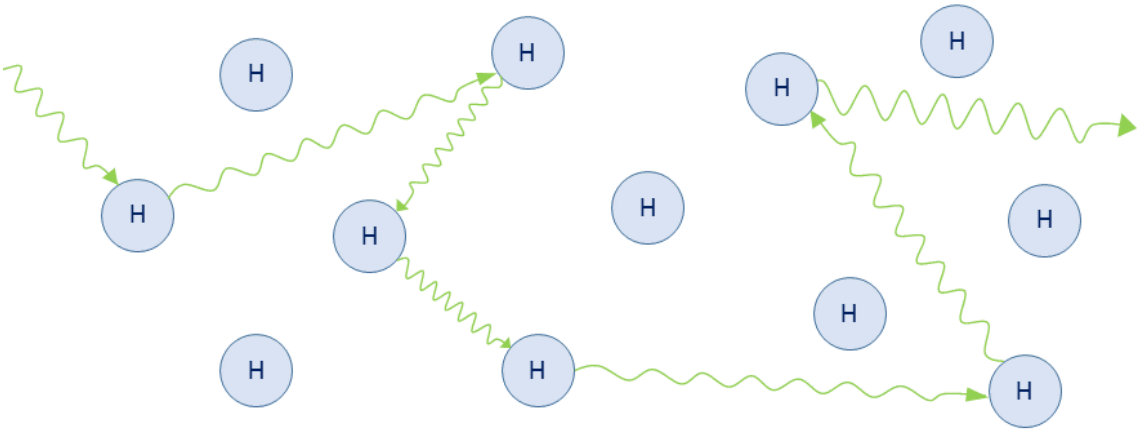

Figure 1.1: **Radiative Transfer Sketch:** A photon being absorbed and re-emitted by Hydrogen atoms.

When a photon is emitted, it travels through the interstellar medium (ISM) of the galaxy. During its path it can encounter another H atom and be absorbed by it. The energy carried by the photon is used to excite the atom and start a re-emission

process, the same way as described before. This photon's scattering can happen several times until it is able to escape the galaxy, as seen in Fig. 1.1. Additionally, as the phenomenon consists of transferring light through scatterings, it is called a radiative transfer process.

If the galaxy is completely static, this process would create a single peak around the natural Ly-α wavelength. Notwithstanding, if now the atoms have a velocity that obeys the dynamics of the galaxy, the re-emitted photon will not have the same wavelength it came with. This is what affects the Ly-α line shape.

These unknown dynamics are what I explore in this work by proposing a new model for a LAE. The model is explained in detail in Chapter 2.

1.2 The Radiative Transfer Code

In order to test this new model I have to know the effect of its parameters in the outgoing Ly-α line. Nonetheless and on the contrary of other areas of science, in astronomy is not possible to do experiments with the objects we observe. It becomes necessary to draw upon programming to explore and test the new models that appear. Then, with the arrivals of new and better observations these models can be reinforced or refuted in time.

In this monograph's case it is then necessary to create a program that simulates a LAE in order to test the model. This means, the code has to take into account the radiative transfer explained in the previous section. This classifies the program as a radiative transfer code. Now, because of the resonant nature of the Ly-α line, the equation that describes a radiative transfer can not be solved analytically. Numerical methods achieved through computation are required. This remarks how important is for these programs to exist.

One radiative transfer code that exists in the literature is CLARA (Code for Lyman Alpha Radiation Analysis). CLARA was created by Forero-Romero et al. [3]. It emulates the Ly-α line of a spherical rotating LAE depending on its mass and velocity. In this work I modify CLARA so the galaxy behaves as in my model.

1.3 Monograph Overview

This monograph is structured as follows. In Chapter 2 I explain the model of rotation and outflows used. In Chapter 3 I present the results of the simulations. In Chapter 4 I compare the results with a LAE observation. In Chapter 5 I present the conclusions and possible future work. Finally, in the Appendix, I present the results of a Ly-α line modeled also with rotation and outflows but with a different implementation.

Chapter 2

Model

LAEs, although not very known, are still galaxies. They are a collection of bodies and matter interacting one with another. This causes particular movements as a whole that should always be present and considered. Two of these main movements are the rotation and expansion.

All bodies in the universe feel a gravitational attraction between them. A galaxy starts forming when some of them start to collapse around their center of mass. However, the matter in the universe is not uniformly distributed. There are some lumps of different masses and at distinct distances around the galaxy. This causes its different parts to be pulled more strongly in some directions. As probably the torques don't balance the galaxy starts to spin in a certain way and with a rotational velocity v_{rot} .

If one considers the rotational velocity of a galaxy plus its gravitational collapsing towards its center of mass, an interesting effect is observed. The initial sphere starts to flatten into a disk, just as our Milky Way [1]. However, a very long time has to pass until this takes place. And in LAEs, because they are very young, the material collapsing is still pseudo uniformly distributed in a spherical shape.

[1] This is the same effect that causes a ball of mass to become a flat pizza when the chef throws it in the air spinning

On another scale, the stars inside this new forming galaxy follow a different time scale. Their duration is much shorter so many supernovas happen during the galaxy's life time. These supreme explosions eject material in all directions. They travel through the body in such a strong way, they can even escape from it. These are called outflows and induce a radial velocity to the galaxy v_{out} .

These 3 considerations leave the idea of a model of LAE, that although simple, considers the main galaxy's dynamics. All of them have been previously proposed by different author, but never combined together. This new model consists of the mixture of them.

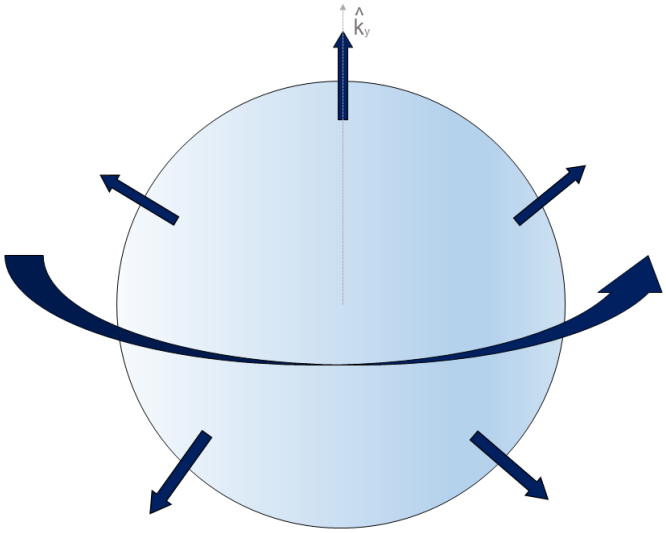

Figure 2.1: **Model:** Spherical LAE with tangential and radial velocity due to rotation and outflows, respectively.

I propose a spherical galaxy composed by H atoms that undergo a solid-body rotation and a radial expansion due to outflows, as seen in Fig. 2.1. In this model the velocity of each H atom is described by components in Eqs. 2.0.1 2.0.2 2.0.3. In these, R is the radius of the sphere; x, y and z are the position of the atom; and the $\mp$ signs in v_x and v_y, respectively, indicate the direction of rotation. This rotation direction goes according to the right hand rule applied to the $\hat{k}$ unit vector

$$v_x = \frac{x}{R} v_{\text{out}} - \frac{y}{R} v_{\text{rot}} \tag{2.0.1}$$

$$v_y = \frac{y}{R} v_{\text{out}} + \frac{x}{R} v_{\text{rot}} \tag{2.0.2}$$

$$v_z = \frac{z}{R} v_{\text{out}} \tag{2.0.3}$$

Apart from these velocities, another key factor needs to be taken into account. This is the mass of the LAE, or in another words, its number of H atoms. For this reason another dimensionless variable is defined, called the optical depth τ_{H} . τ_{H} measures the number of H atoms found if one traces a line from the center of the galaxy, to its edge.

Now the 3 main model parameters are defined: v_{rot} , v_{out} and τ_{H} .

2.1 Photon's Path

In several problems in science it is sometimes really useful to define dimensionless variables of equations. This new formulation has many advantages. For example, now regardless of units, there is always a definition of small. This tends to make the results' analysis much more easier. For this reason, I define a new dimensionless variable x in the model to describe a photon's wavelength.

$$x \equiv \frac{(\nu - \nu_\alpha)}{\Delta\nu_{\text{D}}} \tag{2.1.4}$$

A photon's wavelength can be also expressed as its reciprocal form of frequency ν. This is defined as $\nu = c/\lambda$, where c is the speed of light and λ is the wavelength. So, in Eq. 2.1.4, ν refers to the photon's frequency and $\nu_\alpha = 2.46 \times 10^{15}$ Hz is the Ly-α natural frequency. The denominator $\Delta\nu_{\rm D}$ is defined in Eq. 2.1.5.

$$\Delta\nu_{\rm D} \equiv \nu_\alpha \sqrt{\frac{2kT}{m_p c^2}} \equiv \nu_\alpha \frac{v_{\rm th}}{c} \tag{2.1.5}$$

$\Delta\nu_{\rm D}$ is the Doppler broadening of the Ly-α line. It depends on the neutral gas temperature T or equivalently the thermal velocity $v_{\rm th}$ of the atoms. In the model the temperature is $T = 10^4$K and the thermal velocity is $v_{\rm th} = 12.8\,{\rm km\ s^{-1}}$.

This variable x is now the parameter that defines how the final wavelength of a photon ends up. If $x < 0$, the final frequency $\nu < \nu_\alpha$. This translates to the final wavelength being larger than the Ly-α natural one. The phenomenon is called a redshift in frequency. If, on the contrary, $x > 0$, the photon suffers a blueshift in frequency.

As mentioned before, this is a radiative transfer model. This means that it is necessary to define the way the energy is transfered through the galaxy. For simplicity of the code, the initial emission of photons is taken at the center of the sphere. From here, 100000 photons are emitted with the natural Ly-α wavelength. Then, they start to behave as previously described (See Fig. 1.1). When each photon is re-emitted, its new wavelength depends merely on the H atom velocity. However its new direction of propagation is random.

The individual scattering of all the photons is tracked through the complete 3D Hydrogen distribution. Once each photon escapes the galaxy, its final values are stored: position $\vec{r}$, direction of propagation $\hat{k}$, dimensionless frequency x, and number of scatterings N. When the last photon leaves the galaxy, a histogram of final

x values is created. This plot represents the Ly-α line of the galaxy spectrum.

2.2 Galaxy's Viewing Angle

Is important to note that if we stand next to the galaxy, not all of the photons emitted are going to be observed because some will have directions that could never reach our position. For this reason, it is very important to define viewing angle so that only photons that escape within that range are counted in the spectrum. As seen in Fig. 2.2, only the photons with escaping direction angle θ respect to the rotation axis that belongs to the range $[\theta_{min} - \theta_{max}]$ reach the observer.

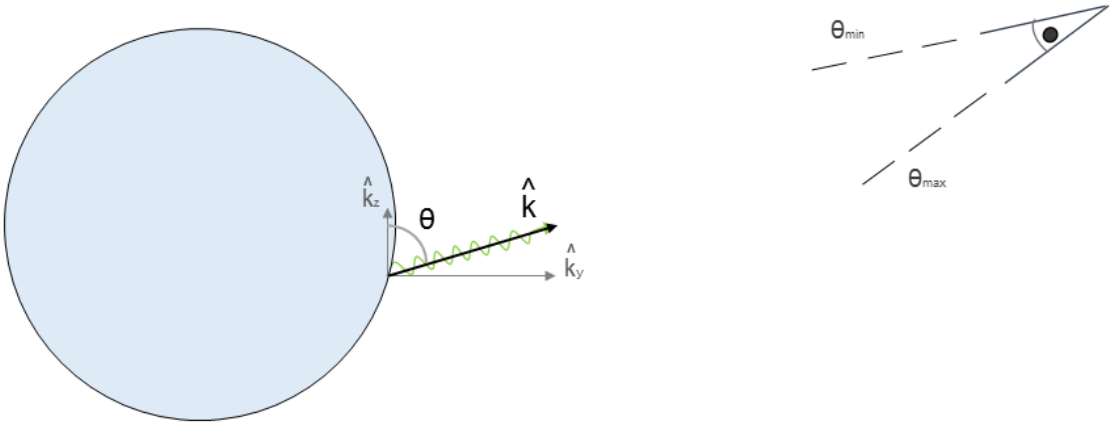

Figure 2.2: **Viewing Angle Sketch:** The galaxy is in the $y - z$ plane perspective and the eye is located at an specific viewing angle of the sphere. Only photons with a direction that enters in his range of vision can enter to the result.

This consideration creates 2 new parameters, the azimuthal angle and the polar angle. However, the galaxy's movement is symmetrical respect to its rotation axis. This implies that the resulting spectrum will not vary depending on the azimuthal angle. This makes all of the photons with azimuthal viewing angle from 0 to 2π have the same result, disregarding the selected polar range. I will choose all of them for statistical reasons. Regarding the polar angle, I will take spectra from 9 different

ranges from 0 to π that are uniform in $\cos(\theta)$ and analyze the influence of this effect as well.

All of the resulting spectra considering the 3 galaxy parameters and the viewing angle are available in the next chapter.

Chapter 3

Results

3.1 Parameters' Intial Values

With the model defined and the code implemented, the following step is to run the simulations. It is then necessary to set values for the parameters.

In order to define the ranges of τ_{H} it is necessary to refer to observations. The literature available offers a value of LAE's Hydrogen mass that goes from $2.7\times10^{8}\mathrm{M}_{\odot}$-$2.7\times10^{9}\mathrm{M}_{\odot}$. These values cause a Hydrogen density of $4\times10^{-4}-4\times10^{-3}$ atoms/cm^3, which finally translates to the ranges of optical depth: $\tau_{\mathrm{H}} = 2\times10^{5} - 2\times10^{6}$. However to consider LAEs that might be more massive, I will extend this range to $\tau_{\mathrm{H}} = 2\times10^{5} - 2\times10^{7}$

When looking at the literature one can find typical values for both v_{rot} and v_{out} . Nonetheless, the combined effect of these two have never been studied on a LAE before. Because of this, I made a mapping of them without concerning of their physical meaning. So, all the combinations of Tab. 3.1 are executed.

The final results are shown in the Appendix A in Figs. A.1, A.2 and A.3. In these three sets of figures it is noted that most of the lines are a single peaks. However, the effect of rotation should create two. Only in few squares the 2 peaks are visible but they are almost insignificant in comparison and there has to be low v_{rot} and

$\tau_{\mathbf{H}}$	v_{rot} (km s^{-1})	v_{out} (km s^{-1})
10^5, 10^6, 10^7	0, 100, 200 ,300	100, 200 ,300

Table 3.1: **Combinations of parameters' values:** Rough estimation to see the effect of each parameter.

$v_{\rm out}$ to obtain them. This means that the outflows effect so much larger than the other one, and in order to compare the influence of both is necessary to lower $v_{\rm out}$. This behavior extends for all the viewing angle ranges.

3.2 Narrowing Parameters' Values

Knowing the typical velocity values for a LAE and that $v_{\rm out}$ has to be much lower than $v_{\rm rot}$, the values of the parameters are narrowed. All of them are registered in Tab. 3.2. Their combinations are executed.

$\tau_{\mathbf{H}}$	v_{rot} (km s^{-1})	v_{out} (km s^{-1})
10^5, 10^6, 10^7	50, 100	5, 10, 15, 20, 25, 50, 75

Table 3.2: **Combinations of parameters' values:** The velocities are now consistent with the LAE's mass and typical properties

From these new sets of spectra I notice that $v_{\rm out} = 50,\ 75$ km s^{-1}still behave as the values of the previous section. The outflows velocity is too large to let another effect be visible. These spectra are also available in the Appendix A in Figs. A.4 A.5 A.6.

On the other side, for the remaining values of $v_{\rm out}$ significants results are obtained. They are shown in Figs. 3.1, 3.3 and 3.2.

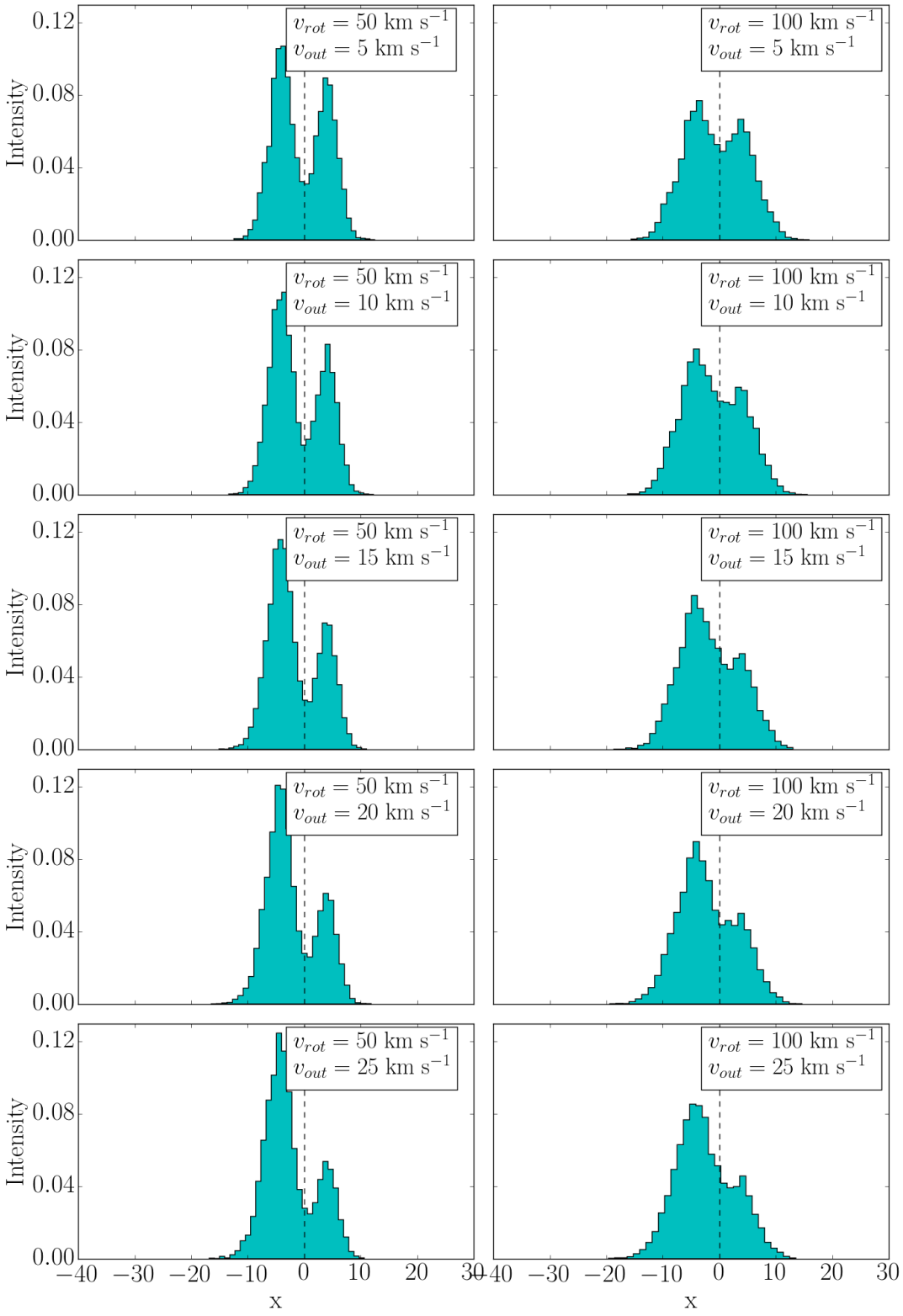

Figure 3.1: **Ly-α profile for $\tau_{\rm H} = 10^5$:** With $v_{\rm rot}$ ranging $50, 100$ km s^{-1}and $v_{\rm out}$ ranging $5, 10, 15, 20, 25$ km s^{-1}. The intensity is in arbitrary units.

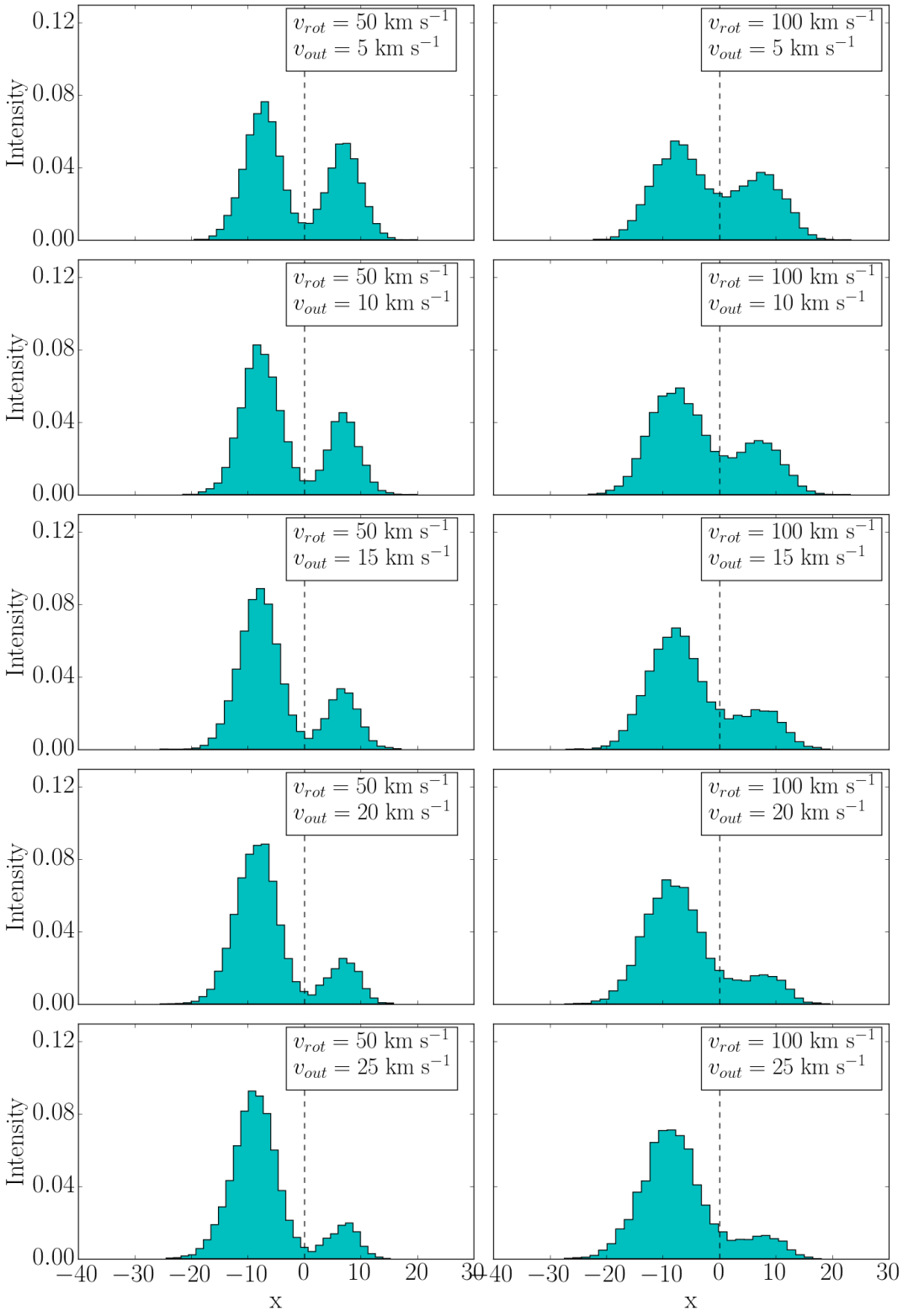

Figure 3.2: **Ly-α profile for $\tau_{\mathrm{H}} = 10^6$:** With v_{rot} ranging $50, 100$ km s^{-1}and v_{out} ranging $5, 10, 15, 20, 25$ km s^{-1}. The intensity is in arbitrary units.

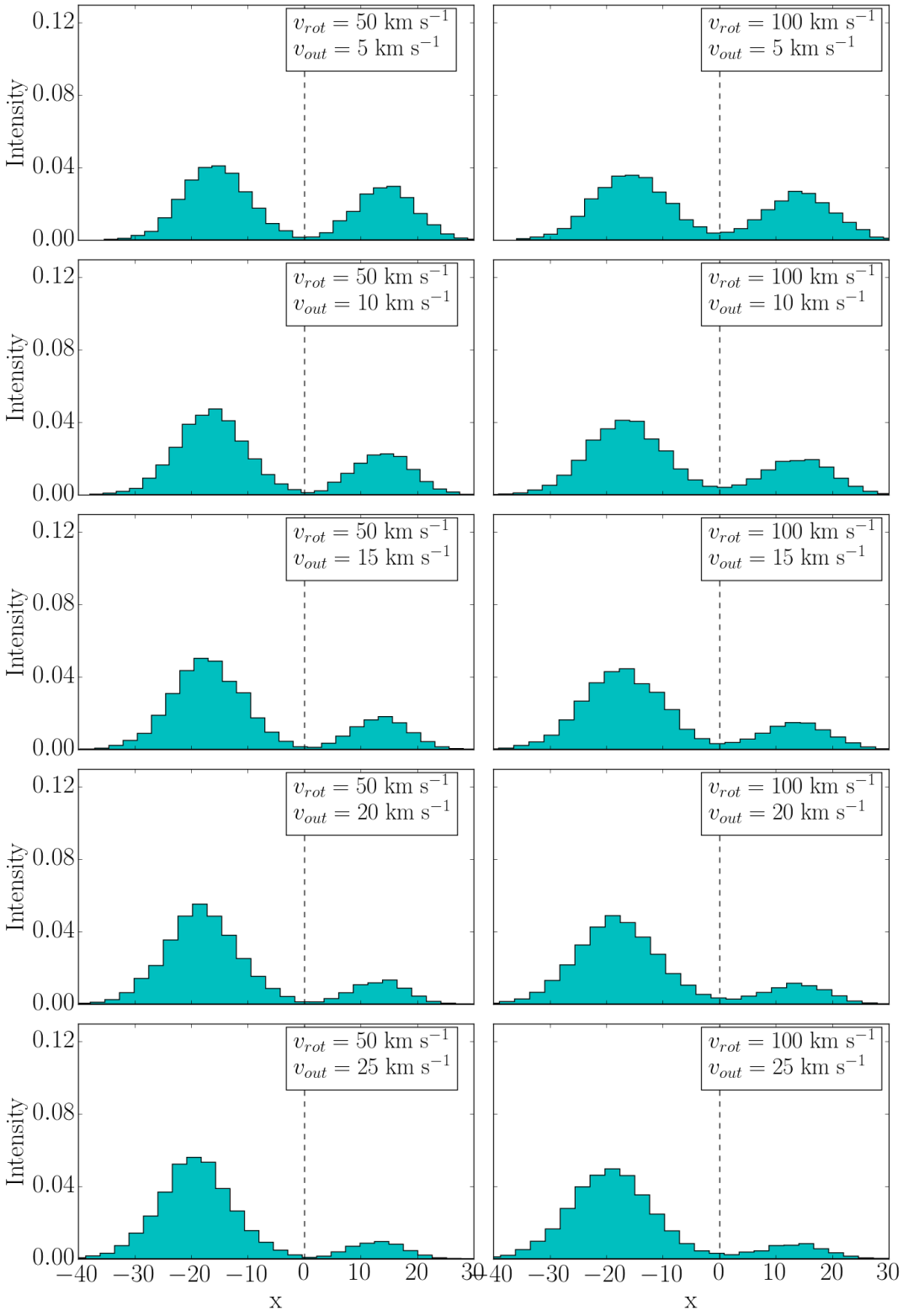

Figure 3.3: **Ly-α profile for $\tau_{\mathrm{H}} = 10^7$:** With v_{rot} ranging $50, 100$ km s^{-1}and v_{out} ranging $5, 10, 15, 20, 25$ km s^{-1}. The intensity is in arbitrary units.

From the figures I can confirm that only a little fraction of v_{rot} , in the radial direction, is necessary to obtain 2 asymmetric peaks. This final spectra are very consistent with LAEs renowned observations.

3.3 Influence of the viewing angle θ

As stated in the preceding chapter, I have to take into account the viewing angle of the galaxy to create the resulting spectra. For all of the parameters' combinations, the effect of θ in the Ly-α line is always the same.

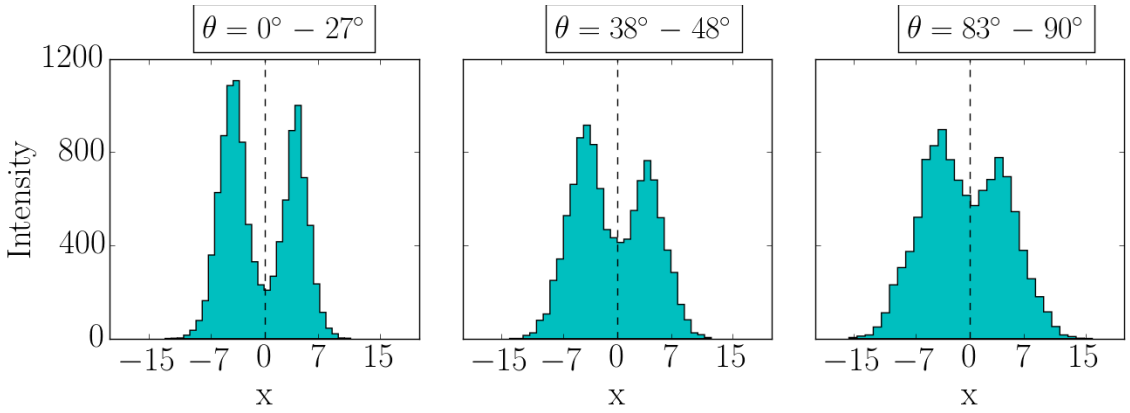

Figure 3.4: **Ly-α profile for different θ:** With $\tau_{\text{H}} = 10^5$, $v_{\text{rot}} = 50$ km s^{-1}and $v_{\text{out}} = 20$ km s^{-1}.The intensity is in arbitrary units.

In order to exemplify, I use the particular case of $\tau_{\text{H}} = 10^5$, $v_{\text{rot}} = 50$ km s^{-1}and $v_{\text{out}} = 20$ km s^{-1}. As seen in Fig. 3.4 it is very clear that the intensity of the valley between the two peaks is increased along with θ. This causes an intensity decrease in the rest of the frequencies, thus a broadening of the line.

It is important to note that I show only the results of a particular range of θ. I choose the range in which I see the galaxy's angular momentum vector going perpendicular to my relative position vector (i.e. $\theta \in [83°, 96°]$). This choice is with the purpose of decreasing the number of plots in the document. However, I ensure

the reader there is an analogous behavior for all of the ranges.

3.4 Morphology of Ly-α line

After obtaining logical and observation-consistent results in the Ly-α line, it is necessary to quantify its morphology. This is done with 3 different factors: the standard deviation (std), the skewness (skw) and a factor sigma of asymmetry (σ_A).

3.4.1 Standard Deviation

In this part I use the std to estimate the dispersion of the frequencies in the Ly-α line. It is important to recall that if the value is close to zero, then the frequencies tend to be very close to their expected value. If it increases, it means the frequencies are spreading to wider ranges.

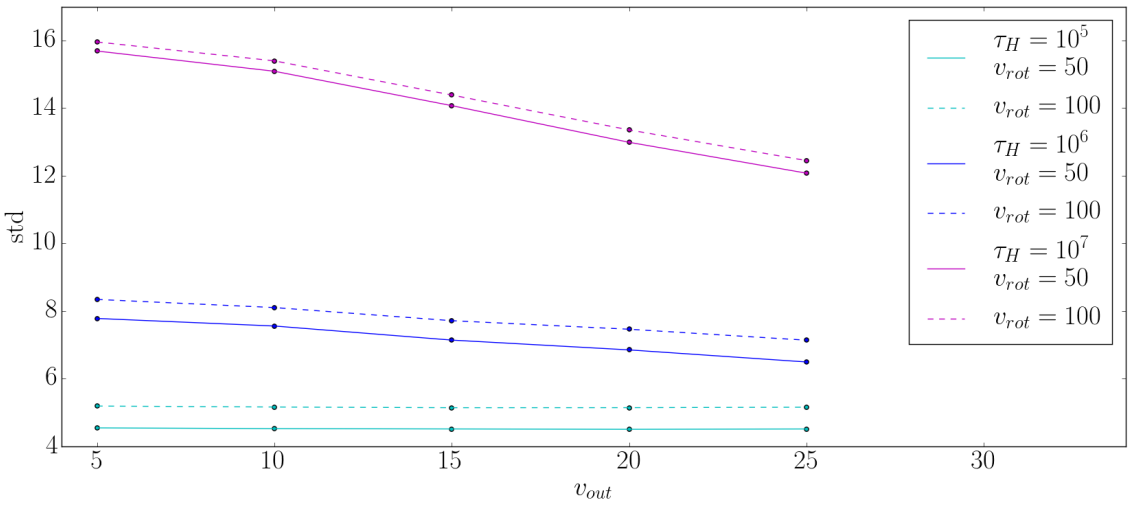

Figure 3.5: **Standard deviation plot for each τ_{H} . The units of v_{rot} and v_{out} are km s^{-1}**

As seen in Fig. 3.5, the standard deviation is inversely proportional to the outflow velocity. Also, the higher the τ_{H} , the more inclined the curves. This implies

that the greater $v_{\rm out}$ is, the less disperse is the Ly-α frequency distribution. This clearly shows that the peaks start merging to one another if $v_{\rm out}$ is increasing.

3.4.2 Skewness

In this part I use the skw to estimate the asymmetry of the Ly-α line. Is important to recall that if the value is greater than zero, there is more weight in the left tail of the line. And on the contrary, if it is less than zero, there is more weight in the right one.

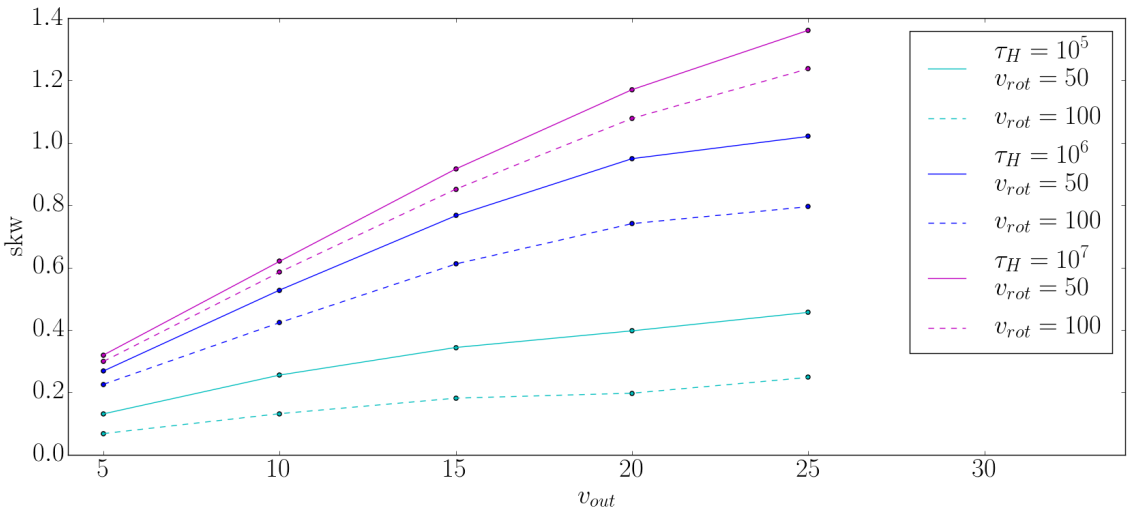

Figure 3.6: **Skewness plot for each $\tau_{\rm H}$. The units of $v_{\rm rot}$ and $v_{\rm out}$ are km s^{-1}**

As seen in Fig. 3.6, the skewness is proportional to the outflow velocity. This implies that the greater $v_{\rm out}$ is, the more asymmetric is the Ly-α frequency distribution.

3.4.3 Sigma of Asymmetry

In this part I use the σ_A factor to estimate in another way the asymmetry of the Ly-α line. This was defined by (MISSING REFERENCE) as follows. The two peaks, the left one and the right one, are fitted with a Gaussian curve. Their standard deviations σ_{left} and σ_{right} are obtained. Then the factor σ_A is:

$$\sigma_A = \frac{\sigma_{right}}{\sigma_{left}} \tag{3.4.1}$$

Is important to recall that if the value is greater than one, the left peak is thiner than the right peak. And if it is less than one, there left peak is wider than the right peak.

(MISSING PLOTS)

3.5 Influences of the free parameters

3.5.1 Influence of the Galaxy Optical Depth: $\tau_{\rm H}$

The influence of $\tau_{\rm H}$ in the Ly-α line can be seen clearly in figures (Fig. A.1 A.2 A.3). What the optical depth causes is that the more $\tau_{\rm H}$ there is, the more redshifted is the line respect to the zero value of x. This result has been previously obtained. So, my results are consistent with literature regarding this parameter.

3.5.2 Influence of the Galaxy Outflow Velocity: $v_{\rm out}$

The influence of $v_{\rm out}$ is very clear since the first run. When this outflows velocity increases, the right peak of the spectrum goes down in intensity until it merges with the left peak. This result has also been previously obtained. So, my results are consistent with literature regarding this other parameter.

3.5.3 Influence of the Galaxy Rotation Velocity: $v_{\rm rot}$

The influence of $v_{\rm rot}$ is slightly clear because of the giant impact $v_{\rm out}$ has. However it is noticeable that the Ly-α line broadens and lowers intensity when the rotation velocity increases. This effect has been less studied in literature. Only Garavito et al. [4] has simulated its effect, but our results are consistent.

Chapter 4

Discussion

4.1 Comparison with an observation

Kulas.

4.2 Importance of this result

No one has tried this combination of rotation and outflows velocity before. These combinations of values make a lot more sense, recalling that v_{out} is caused mainly by ejection of material out the galaxy. It is then common and normal that a galaxy rotates faster than it expands, not the opposite.

Many authors that only include the outflows effect are able to fit observational spectra but with a very large magnitude of v_{out} . And others that include the rotational effect are able to obtain the two peaks but not their asymmetry. The new model proposed in this monograph can cause both of these effects with typical LAE's values.

4.3 Future work

Non central emission.

Chapter 5

Conclusions

Here go the conclusions....

Chapter 6

Bibliography

[1] Fernando Pérez and Brian E. Granger. Ipython: a system for interactive scientific computing. *Computing in Science and Engineering*, 9(3):21–29, May 2007.

[2] J. D. Hunter. Matplotlib: A 2d graphics environment. *Computing In Science & Engineering*, 9(3):90–95, 2007.

[3] J. E. Forero-Romero, G. Yepes, S. Gottlöber, and F. Prada. Modelling the fraction of Lyman break galaxies with strong Lyman α emission at $5 \leq z \leq 7$. *MNRAS*, 419:952–958, January 2012.

[4] J. N. Garavito-Camargo, J. E. Forero-Romero, and M. Dijkstra. The Impact of Gas Bulk Rotation on the Lyα Line. *ApJ*, 795:120, November 2014.

[5] A. Verhamme, D. Schaerer, and A. Maselli. 3D Lyα radiation transfer. I. Understanding Lyα line profile morphologies. *A&A*, 460:397–413, December 2006.

[6] A. Orsi, C. G. Lacey, and C. M. Baugh. Can galactic outflows explain the properties of Ly α emitters? *MNRAS*, 425:87–115, September 2012.

[7] J. P. Walker-Soler, E. Gawiser, N. A. Bond, N. Padilla, and H. Francke. Present-day Descendants of z = 3 Lyα-emitting Galaxies in the Millennium-II Halo Merger Trees. *ApJ*, 752:160, June 2012.

[8] D. Narayanan, M. Bothwell, and R. Davé. Galaxy gas fractions at high redshift: the tension between observations and cosmological simulations. *MNRAS*, 426:1178–1184, October 2012.

[9] Planck Collaboration, P. A. R. Ade, N. Aghanim, M. Arnaud, M. Ashdown, J. Aumont, C. Baccigalupi, A. J. Banday, R. B. Barreiro, J. G. Bartlett, and et al. Planck 2015 results. XIII. Cosmological parameters. *ArXiv e-prints*, February 2015.

Appendix A

Results' Figures

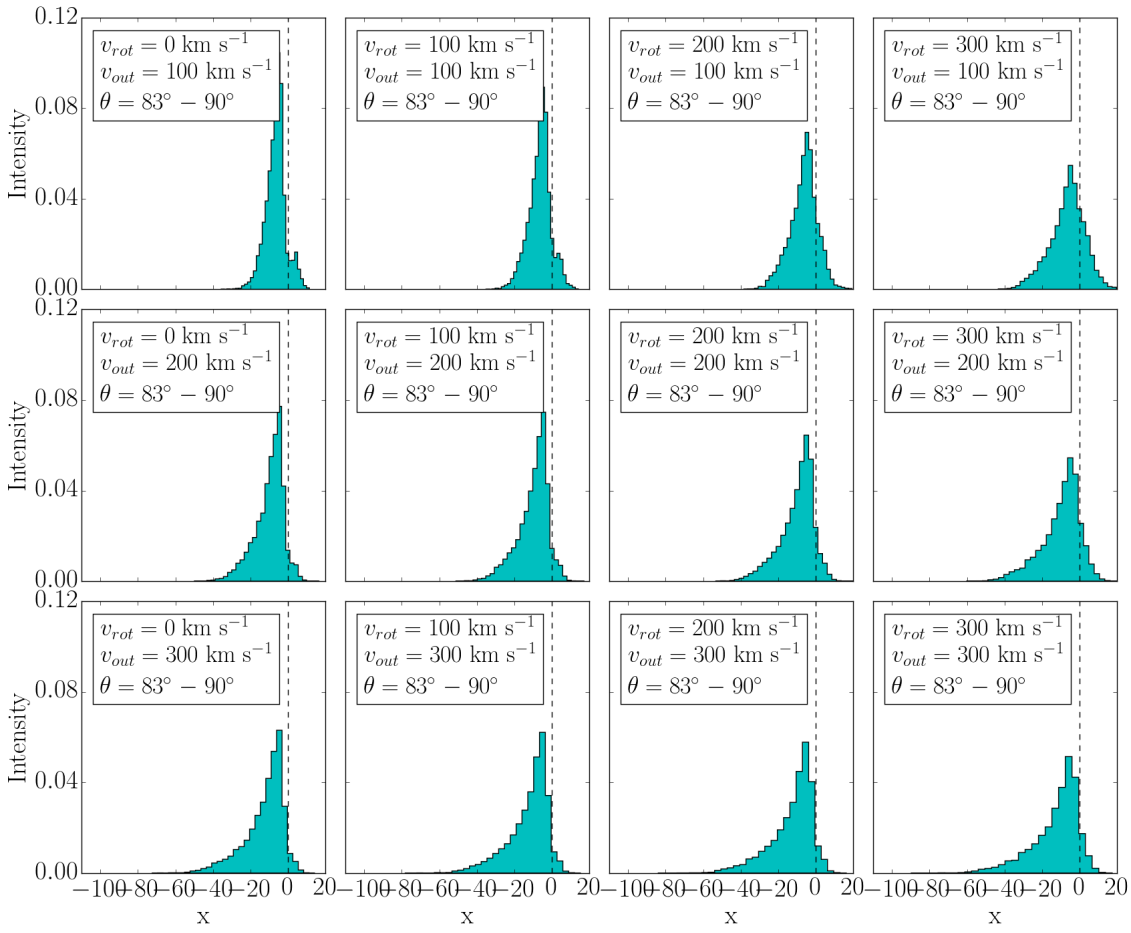

Figure A.1: **Ly-α profile for $\tau_{\rm H} = 10^5$:** With $v_{\rm rot}$ ranging $0, 100, 200, 300$ km s^{-1}and $v_{\rm out}$ ranging $100, 200, 300$ km s^{-1}.

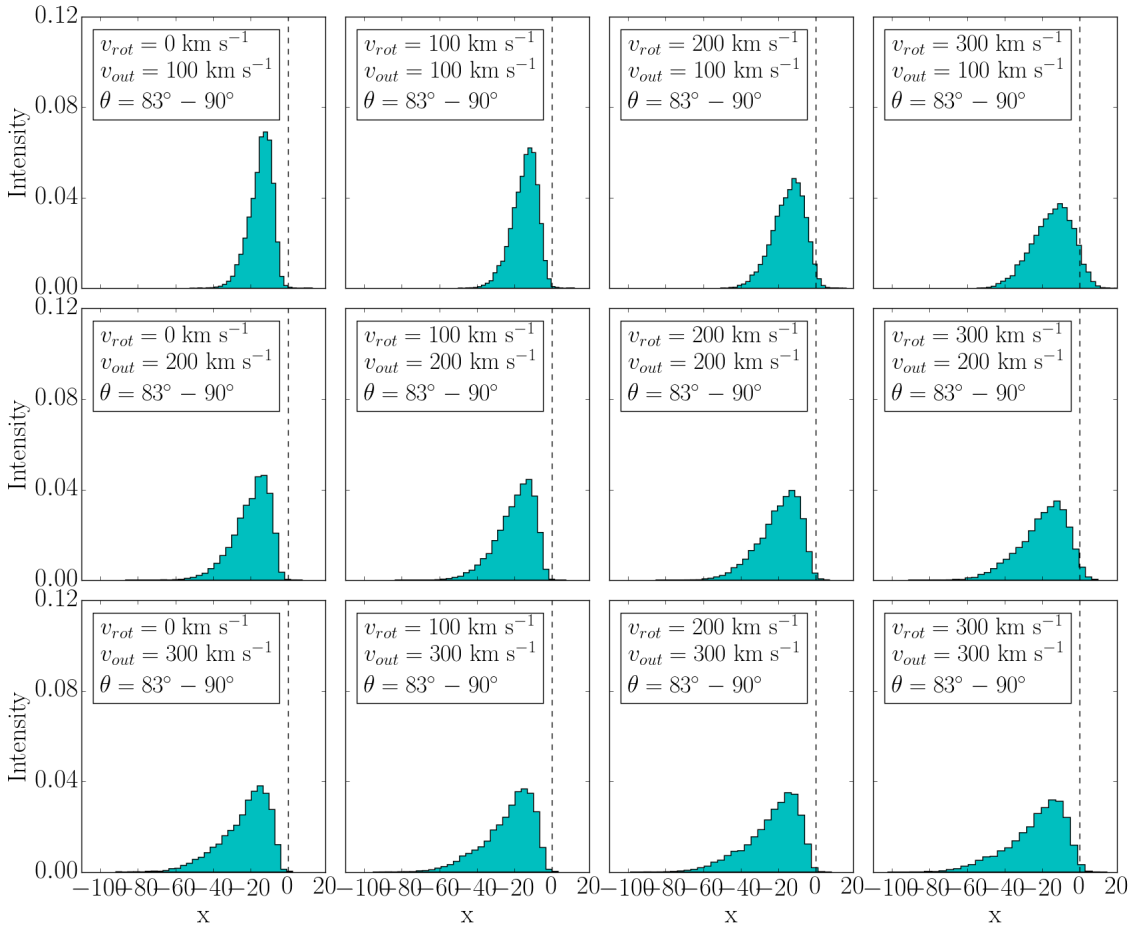

Figure A.2: **Ly-α profile for $\tau_{\rm H} = 10^6$:** With $v_{\rm rot}$ ranging $0, 100, 200, 300$ km s^{-1}and $v_{\rm out}$ ranging $100, 200, 300$ km s^{-1}.

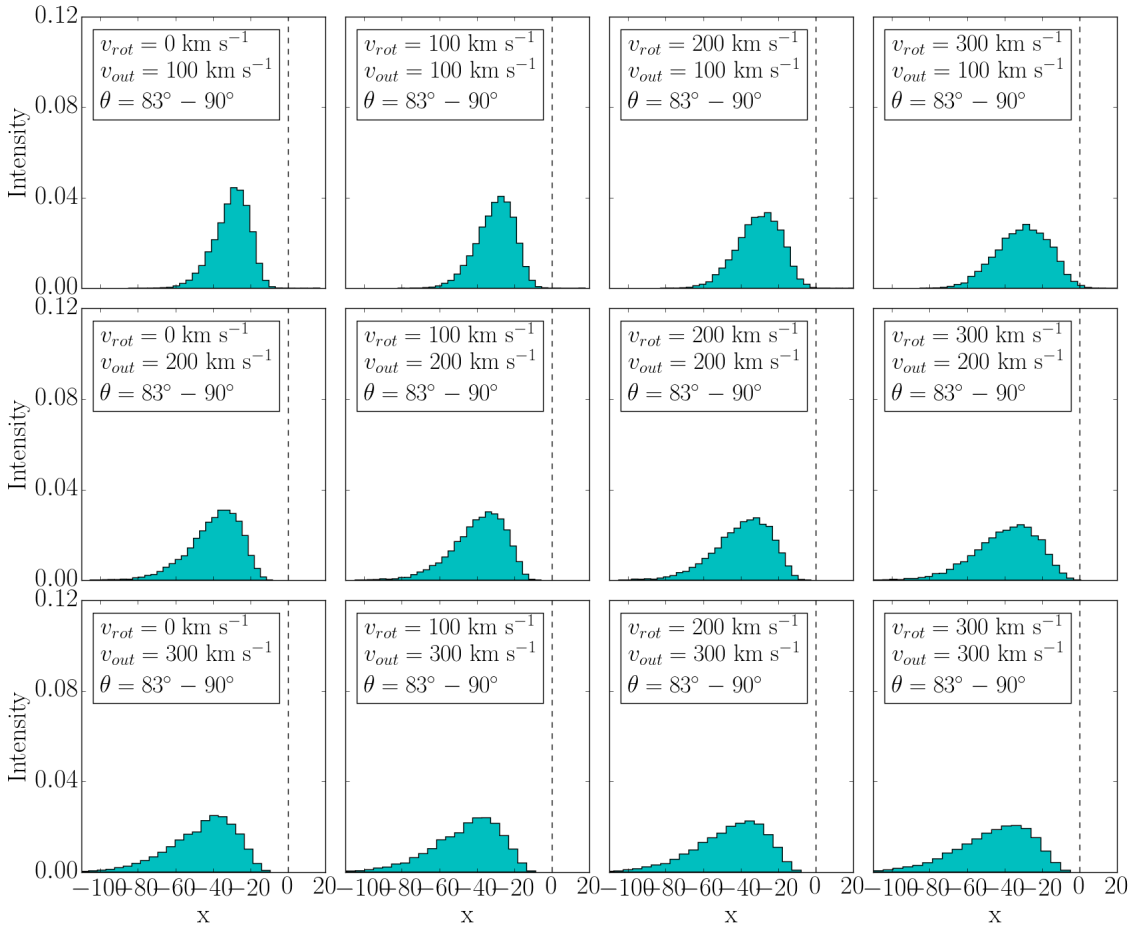

Figure A.3: **Ly-α profile for $\tau_{\rm H} = 10^7$:** With $v_{\rm rot}$ ranging $0, 100, 200, 300$ km s^{-1}and $v_{\rm out}$ ranging $100, 200, 300$ km s^{-1}.

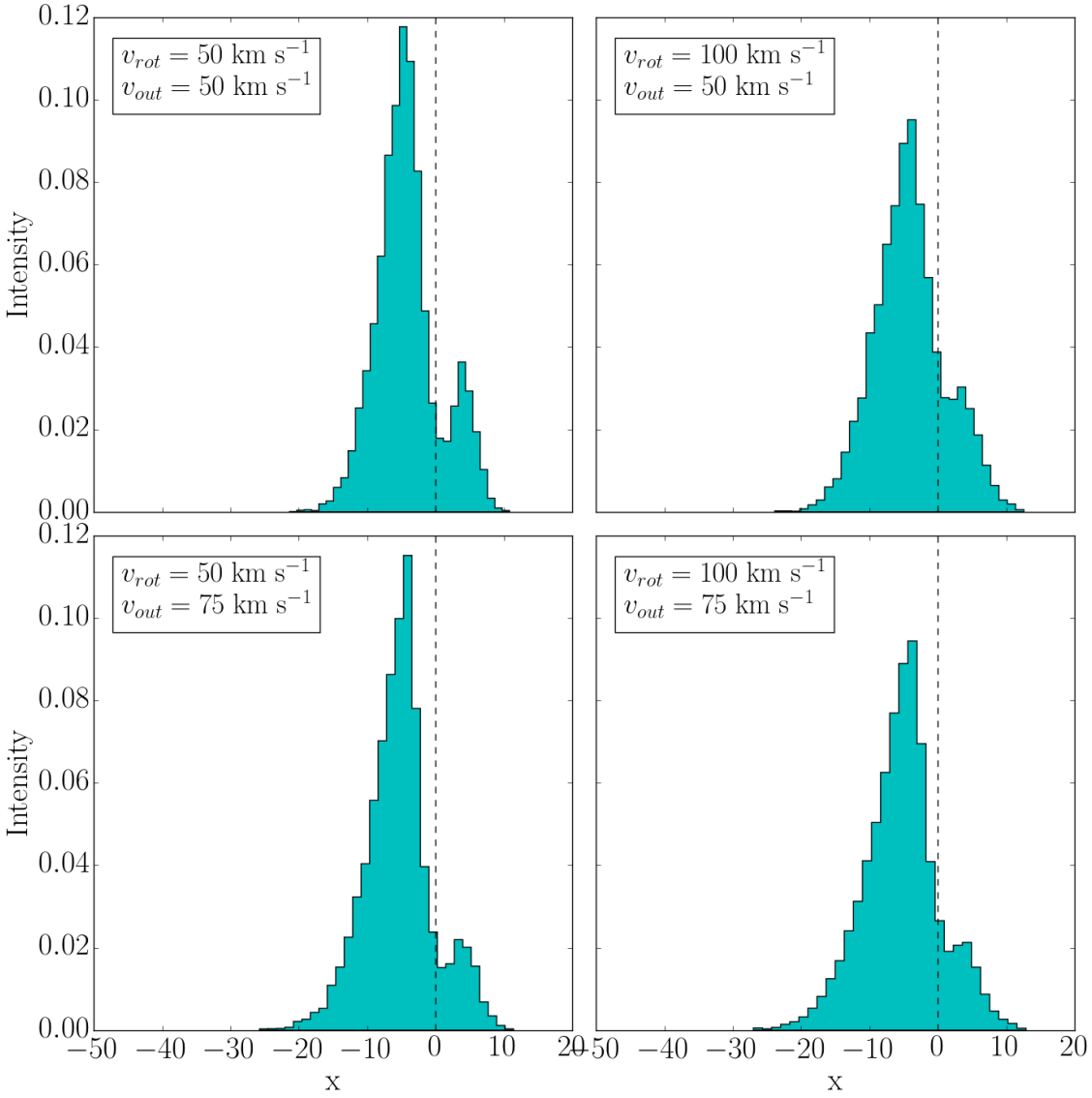

Figure A.4: **Ly-α profile for $\tau_{\rm H} = 10^5$:** With $v_{\rm rot}$ ranging $50, 100$ km s^{-1}and $v_{\rm out}$ ranging $25, 50, 75$ km s^{-1}.

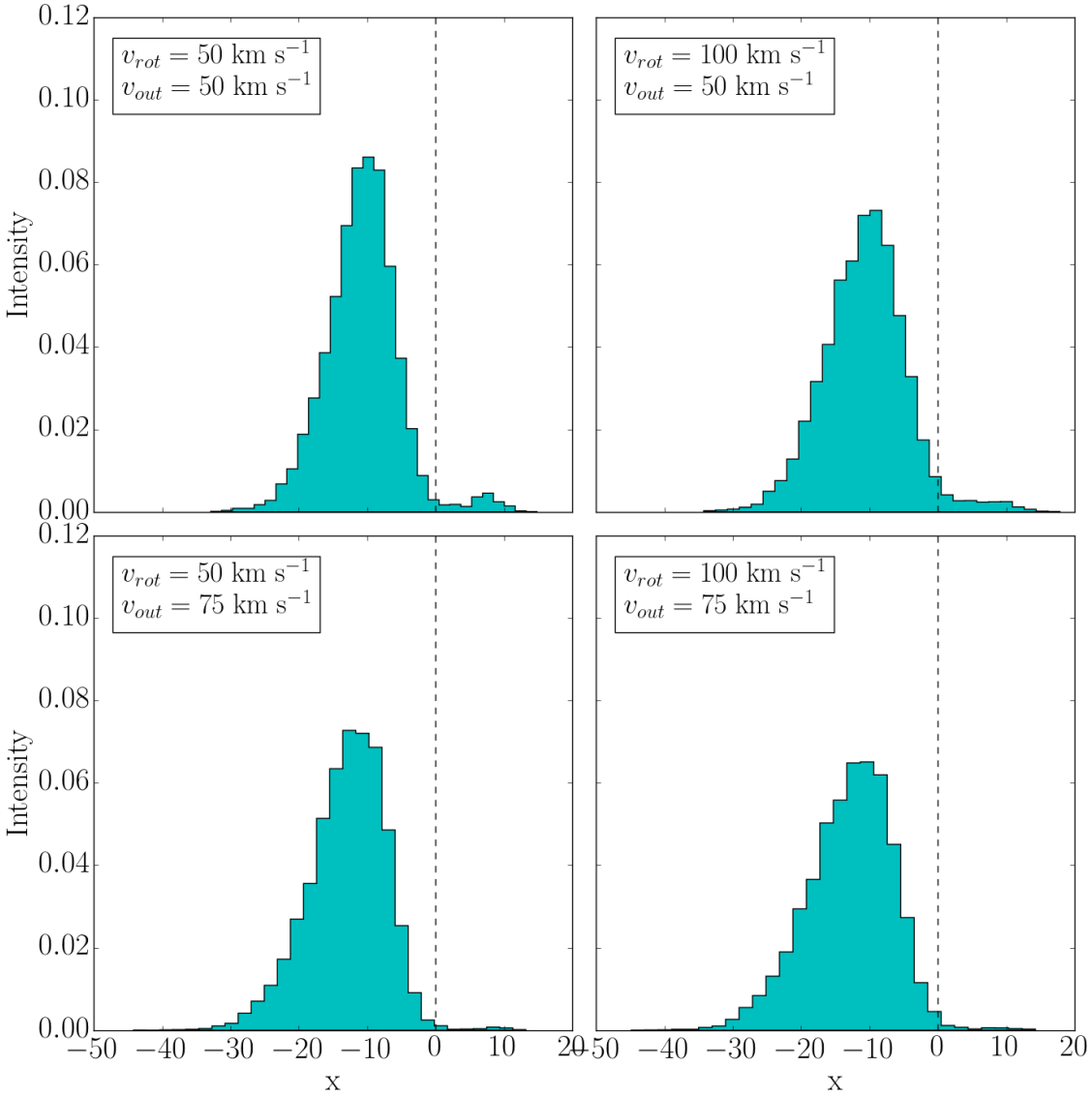

Figure A.5: **Ly-α profile for $\tau_{\rm H} = 10^5$:** With $v_{\rm rot}$ ranging $50, 100$ km s^{-1}and $v_{\rm out}$ ranging $25, 50, 75$ km s^{-1}.

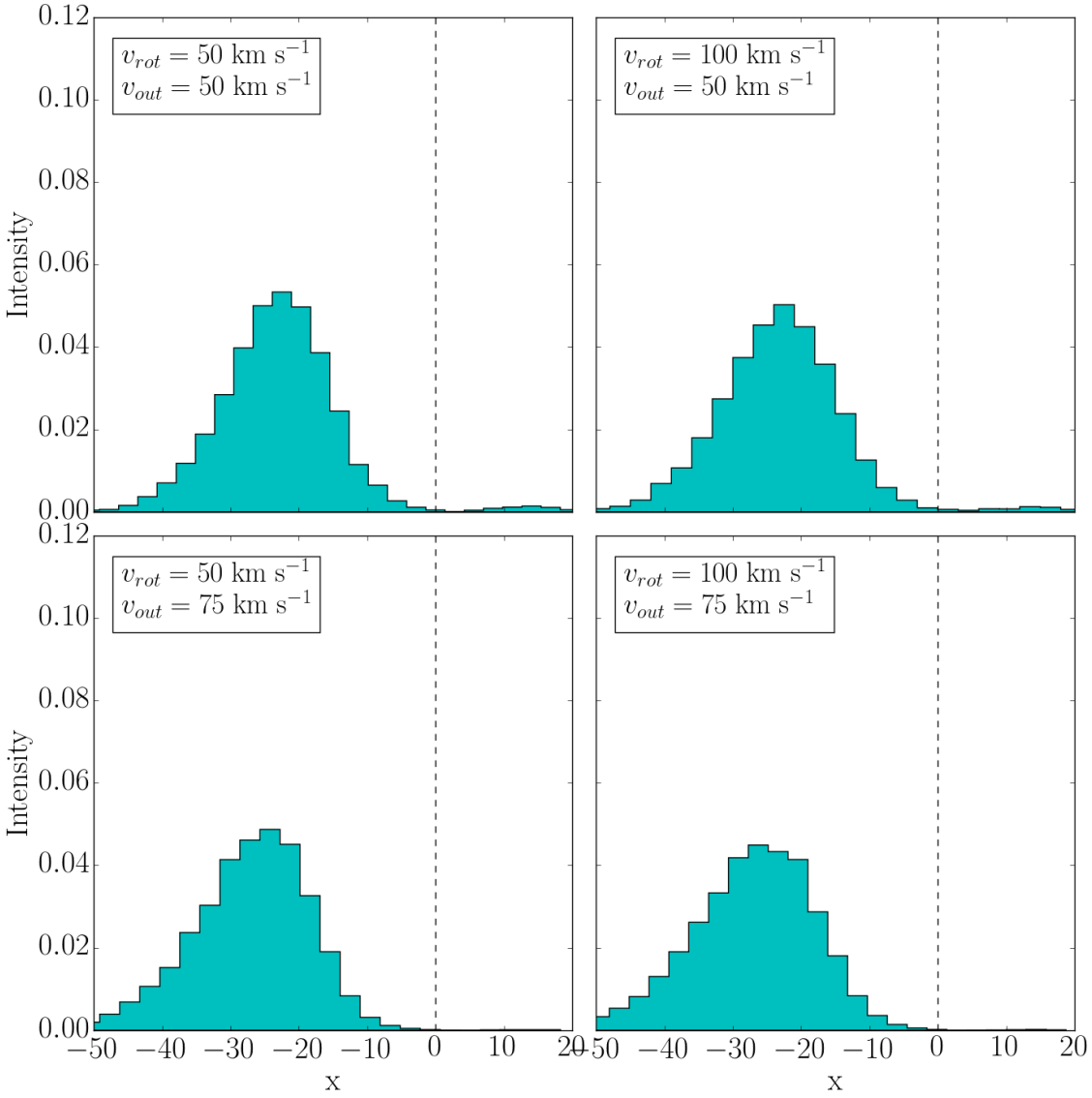

Figure A.6: **Ly-α profile for $\tau_{\rm H} = 10^5$:** With $v_{\rm rot}$ ranging $50, 100$ km s^{-1}and $v_{\rm out}$ ranging $25, 50, 75$ km s^{-1}.

Appendix B

Rotation + Thin Shell Outflow

In this section we describe the two different models that together are used to reproduce a real and consistent Ly-α profile. The first one is a rotation model for the galaxy and the second is a thin shell model for the outflow.

B.1 Rotation Model

We use the simplified rotation model developed by [4] in which a rotating galaxy is modeled as a solid rotating sphere, with a homogeneous mixture of hydrogen and dust. Photons can be initially at the center or can be homogeneously distributed inside the sphere. The equations governing this solid-body rotation sphere in which the axis of rotation is defined to be align with the z-axis are:

$$v_x = -\frac{y}{R} V_{\max}, \tag{B.1.1}$$

$$v_y = \frac{x}{R} V_{\max}, \tag{B.1.2}$$

$$v_z = 0, \tag{B.1.3}$$

Where R is the radius of the sphere and $V_{\max}$ is the linear velocity at the sphere's surface. The minus/plus sign in the x/y-component of the velocity indicates the direction of rotation. In this case we take the angular velocity in the same direction as the $\hat{k}$ unit vector.

In this work we use the analytical expression for rotation derived in [4] where a rotating sphere can be seen as a static sphere in the laboratory frame with a bulk velocity difference in each surface element with respect to a distant observer. With the previous analysis the outcoming spectra can be expressed as:

$$J(x,i) \approx 2\pi \int_0^R db \quad b \int_0^{2\pi} d\phi \quad J(x,b,\phi,i), \tag{B.1.4}$$

Where $J(x,b,\phi,i)$ is the spectrum of the flux emerging from the surface at point (b,ϕ) and is expressed as:

$$J(x,b,\phi,i) = \frac{\sqrt{\pi}}{\sqrt{24}a\tau_0}\left(\frac{(x-x_{\rm b})^2}{1+\cosh\left[\sqrt{\frac{2\pi^3}{27}}\frac{|(x-x_{\rm b})^3|}{a\tau_0}\right]}\right) \tag{B.1.5}$$

B.2 Thin Shell Outflow Model

We use an outflow model that follows the characteristics put described in [5] with the code presented in [6]. The outflow consists of an isothermal, spherical flow expanding at constant velocity $v_{\rm out}$. The outflow is empty inside the shell's inner radius R_{in} and reaches out to an external radius R_{out}. The relationship between these two radii is parameterized by $R_{in} = f_{th}R_{out}$, with $f_{th} = 0.9$ as the fiducial value. The temperature of the medium is assumed constant and equal to $T = 10^4 K$ which sets

the velocity dispersion of Maxwell-Boltzmann distributions to $v_{\rm th} = 12.84$ km s^{-1}.

The gas has an homogeneous Hydrogen number density inside the flow. The total mass inside the shell is parameterized by its column density

$$N_H = \frac{X_H M_{shell}}{4\pi m_H R^2{}_{out}}, \tag{B.2.6}$$

where M_{shell} is the outflow mass, m_H is the mass of the hydrogen atom and $X_H = 0.74$ is the fraction of hydrogen in the cold gas.

The outflow also includes dust homogeneously mixed with the gas. The dust optical depth τ_d is parameterized by the metallicity of the cold gas $\langle Z_{cold} \rangle$:

$$\tau_d ???? \langle Z_{cold} \rangle \tag{B.2.7}$$

B.3 Joint Model

The joint model consists of combining the two models that were just explained. A rotating spherical galaxy is placed at the center with a thin shell outflow surrounding it as seen in Fig. B.1. What happens is that the photons that escaped the galaxy enter now into the outflow with the same radial direction that they came out with. At the end only a fraction of those manage to get out of the outflow and their wavelengths are measured to find the final spectrum.

In order to simulate all the possible cases we set some key parameters for the program to vary, and some others fixed which are defined by the characteristics of LAEs. This are chosen as follows.

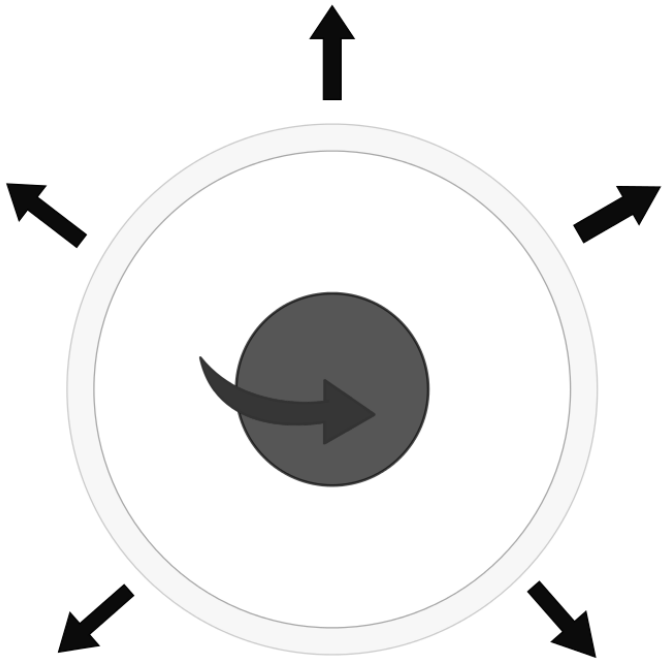

Figure B.1: **Model:** A central rotating galaxy surrounded by an expanding thin shell outflow.

B.4 Galaxy Parameters

Our aim is to provide a realistic baseline to compare against observations of LAES at $z \sim 3$. It has been found by analysis of the abundance and angular correlation function that LAES reside in DM halos of masses in the range $10^{10} - 10^{11} M_{\odot}$[7]. This mass range corresponds to maximum circular velocities in the range $60 - 125\,\mathrm{km\ s^{-1}}$and a median halo scale radius of 15kpc. [1].

These galaxies have gas fractions close to 20% ([8]). We approximate that the hydrogen content is 20% the total baryonic content from the cosmological baryon to dark matter abundances $\Omega_b/\Omega_{dm} = 0.1825$ ([9]), multiplied by a primordial Hydrogen fraction of 0.75. All these considerations gives us hydrogen masses in the range $2.7 \times 10^8 - 2.7 \times 10^9 M_{\odot}$.

These choices give us a range for the number density of Hydrogen atoms of

[1] These results were found using the N-body data available in `www.cosmosim.org`

$4 \times 10^{-4} - 4 \times 10^{-3}$ atoms cm^{-3}. With a Lyman-α cross section at the line center of $\sigma_H = 1.0 \times 10^{-14}$ cm^2 we finally obtain that the optical depth from the cloud's center should be in the range $\tau = 2 \times 10^5 - 2 \times 10^6$.

From these constraints we chose to model two kinds of central galaxies in the extremes of these distributions. The first has $\tau = 2 \times 10^5$ and a raotational velocity of 60 km s^{-1}. The second has $\tau = 2 \times 10^6$ and a rotational velocity of 125 km s^{-1}.

For the first stage there are two fixed parameters: the optical depth $\tau = 10^8$ and the galaxy viewing angle $\theta_{gal} = 90°$. For the second stage there is one fixed parameter: the metallicity of the outflow $Z = -4.0$. This 3 fixed values are selected because the characteristics of observed LAEs, especially their low mass and their highest star formation rate of all.

We have then 3 parameters left that are going to vary along a wide range. These are: the galaxy rotation velocity $v_{\rm rot}$, the outflow hydrogen column density n_H and the outflow expanding velocity $v_{\rm out}$.

$v_{\rm rot}$ covers 3 different angles: 20 km s^{-1}, 100 km s^{-1}and 200 km s^{-1}. $\log n_H$ takes 41 different values from 20.0 to 22.5. And $v_{\rm out}$ covers 5 equidistant velocities from 100 km s^{-1}to 500 km s^{-1}.

The results of this project consist of emulating a LAE spectrum basing on its physical characteristics defined by the 3 free parameters we stated before. When defined the combination of those three.

In the following section each free parameter is explained deeper.

In order to study the influence of each of the three free parameters, we fix two of them and see how the final spectrum varies along the other one left. In each case we will state these changes.

B.4.1 Influence of the Galaxy Rotation Velocity: v_{rot}

If one sets fixed outflow v_{out} and $\log n_H$ in each case the rotation velocity has the same effect: it increases proportionally the intensities. However this change is not that significant. The resulting spectra are completely the same, but enlarged vertically by a small factor. Fig. B.2 helps visualize this effect in a better way.

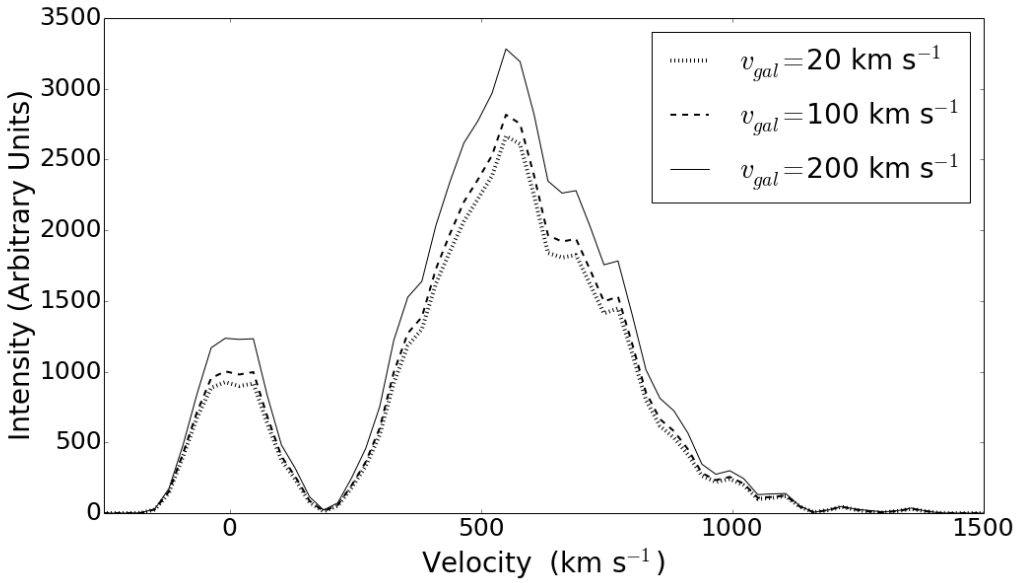

Figure B.2: **Influence of Galaxy Rotation Velocity:** The values of the fixed parameters are $v_{\mathrm{out}} = 100$ km s^{-1}and $\log n_H = 20.9375$. The 3 possible velocities are shown in the plot with different line styles. The increase is visible as well as its small enlargement factor.

B.4.2 Influence of the Outflow Hydrogen Column Density: $\log n_H$

The effect of the $\log n_H$ is the creation of 2 peaks: the left one very thin, tall and pronounced, and the right one very wide, small and soften. When the $\log n_H$ is in-

creased, the left peak starts to decrease while mixing with the right one, decreasing their height ratio until the left peak completely disappears. The resulting spectrum, with high column density, is a wide single mountain with intensity significantly less than at the beginning. Fig. B.3 helps visualize this effect in a better way.

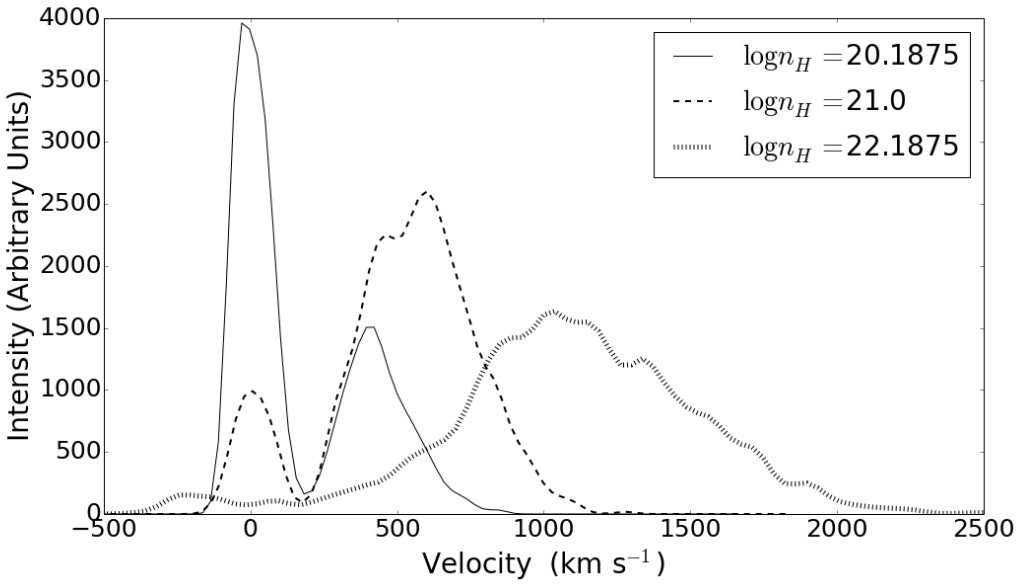

Figure B.3: **Influence of Outflow Hydrogen Column Density:** The values of the fixed parameters are $v_{\rm out} = 100$ km s^{-1}and $v_{\rm rot} = 100$ km s^{-1}. There are three stages of the $\log n_H$ value shown: initial, intermediate and final, with the values shown on the plot.

B.4.3 Influence of the Outflow Expanding Velocity: $v_{\rm out}$

The effect of this parameter consists in a shift of the initial spectrum in the column density. The more $v_{\rm out}$ the outflow has, the more the spectrum simulates the previous velocity but with a greater $\log n_H$. If one compares with Fig. B.3 the similarities are really clear.

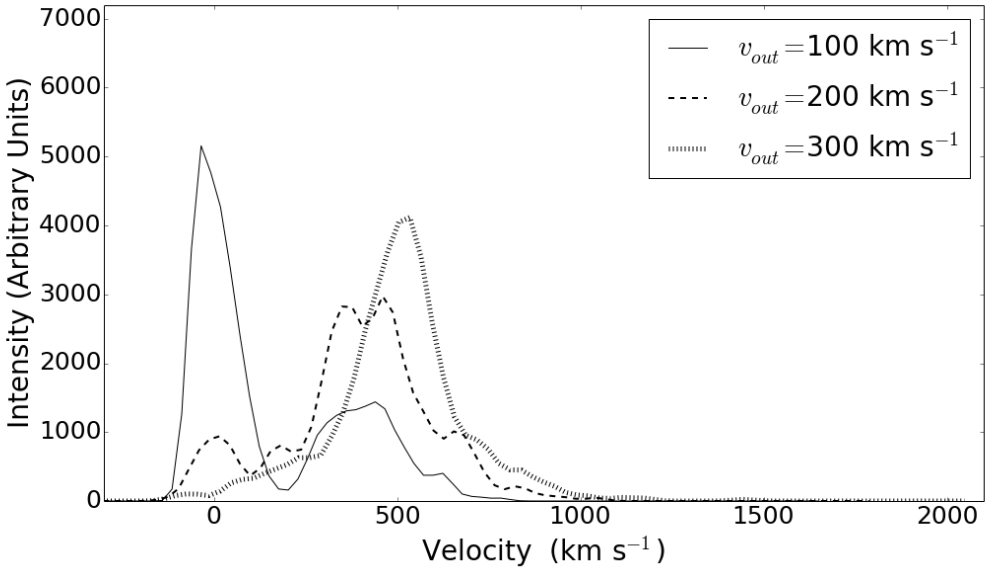

Figure B.4: **Influence of Outflow Expanding Velocity:** The values of the fixed parameters are $\log n_H = 20.125$ and $v_{\rm rot} = 100$ km s^{-1}.

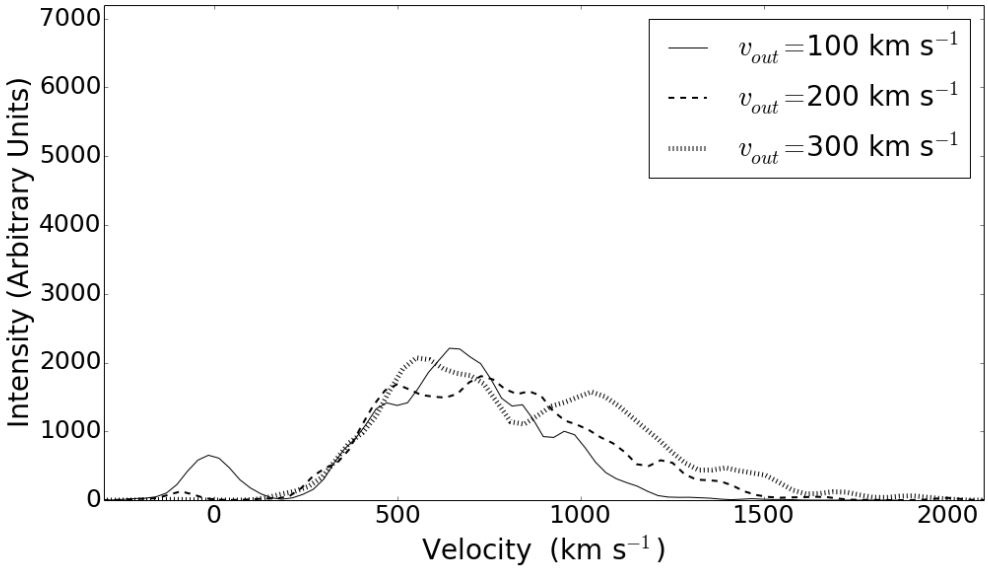

Figure B.5: **Influence of Outflow Expanding Velocity:** The values of the fixed parameters are $\log n_H = 21.25$ and $v_{\rm rot} = 100$ km s^{-1}.